AD NUMBER
ADB257882
LIMITATION CHANGES
TO: **Approved for public release; distribution is unlimited.**
FROM: **Distribution: Further dissemination only as directed by National Aeronautics and Space Administration, Washington, DC, DEC 1950, or higher DoD authority.**
AUTHORITY
NASA TR Server website

NATIONAL ADVISORY COMMITTEE FOR AERONAUTICS

TECHNICAL NOTE 2223

INVESTIGATION OF THE FLOW THROUGH A SINGLE-STAGE TWO-DIMENSIONAL NOZZLE IN THE LANGLEY 11-INCH HYPERSONIC TUNNEL

By Charles H. McLellan, Thomas W. Williams, and Ivan E. Beckwith

Langley Aeronautical Laboratory
Langley Field, Va.

Washington
December 1950

NATIONAL ADVISORY COMMITTEE FOR AERONAUTICS

TECHNICAL NOTE 2223

INVESTIGATION OF THE FLOW THROUGH A SINGLE-STAGE TWO-DIMENSIONAL NOZZLE IN THE LANGLEY 11-INCH HYPERSONIC TUNNEL

By Charles H. McLellan, Thomas W. Williams, and Ivan E. Beckwith

SUMMARY

Flow surveys have been made in the second of several nozzles to be investigated in the Langley 11-inch hypersonic tunnel. The single-stage, two-dimensional nozzle was designed by the method of characteristics for a Mach number of 7.08 without boundary-layer corrections.

The test results show that reasonably uniform flow at an average Mach number of about 6.86 was obtained in a central region of the stream at the test section. This region had a cross section nearly 5 inches square and had a deviation from uniform flow of less than 1 percent in Mach number and 0.3° in flow angle. An increase in Mach number of about 3 percent occurred during test runs of about 60 seconds duration because of distortions of the boundaries at the first minimum due to nonuniform heating of the nozzle blocks during the tests.

INTRODUCTION

The increase in operating speeds and altitudes of pilotless aircraft has created a need for basic aerodynamic data in the hypersonic speed range. In order to provide such data and also to investigate the problems involved in generating uniform hypersonic flows, an 11-inch hypersonic wind tunnel has been placed in operation at the Langley Aeronautical Laboratory.

Two of several proposed nozzle designs for this tunnel have been tested: a two-stage, Mach number 6.98 nozzle and a single-stage, Mach number 7.08 nozzle. The characteristics of the two-stage nozzle are presented in reference 1. The present paper is concerned with the single-stage nozzle; the results of the calibration surveys are presented and some of the problems and peculiarities of this nozzle are discussed.

SYMBOLS

M	Mach number
p_o	settling-chamber pressure
T_o	settling-chamber temperature, degrees Rankine
T_o'	local stagnation temperature, degrees Rankine
p_1	stream static pressure
p_w	wall static pressure
p_t	measured impact pressure
ϵ_h	flow angle in horizontal plane, positive in direction of increasing Y
ϵ_v	flow angle in vertical plane, positive in direction of increasing Z
γ	ratio of specific heats (1.400 used throughout)
X,Y,Z	coordinate axes
δ^*	boundary-layer displacement thickness

APPARATUS

General description.- The tunnel and equipment used in the operation of this nozzle have been described in detail in reference 1. Briefly, the tunnel is of the intermittent type with a high-pressure tank and a vacuum tank of capacities of 400 and 12,000 cubic feet, respectively. A heat exchanger is used to provide stagnation temperatures up to 1300° R. The heat exchanger used in the present tests incorporated steel tubing in place of the copper tubing previously used. The copper-oxide scale mentioned in reference 1 was thus eliminated.

A variable-area supersonic diffuser has been installed since the completion of the tests with the two-stage nozzle. Its effect on the operation of the tunnel is to increase the length of a typical run from about 30 seconds to a maximum of about 90 seconds.

Another change affecting the operation of the tunnel is the installation of a pressure regulator valve upstream of the heat exchanger. The valve could be set so as to maintain a constant settling-chamber pressure throughout a run in the range from approximately 2 to 28 atmospheres.

Nozzle.- The nozzle contour was designed by the method of characteristics. No correction for boundary layer was made. The characteristics net for the nozzle was designed to expand the flow in two dimensions to a Mach number of 7.08. The test section was 10.51 inches high, and thus the first-minimum or throat height was 0.096 inch. The width of the nozzle was 9.95 inches. A view of the nozzle with the side plate removed is given in figure 1, which illustrates the small relative size of the throat. The usual method of design was used, wherein the arbitrary part of the nozzle contour was formed by a faired curve through the midpoints of 14 straight-line wall increments. Each increment was turned 2° outward with respect to the preceding one and had a fixed projected length of one-half the throat height. The calculated contour ordinates are given in table I.

The nozzle blocks were machined to an accuracy of the order of 0.001 inch; however, a permanent warpage of the nozzle blocks of as much as 0.005 inch has since been observed. The nozzle is of fabricated construction as shown in figure 2. The support members and side plates are made of plain carbon steel but the contoured walls are of stainless steel to avoid corrosion.

INSTRUMENTATION

The instruments used for obtaining the flow measurements in this nozzle are in most respects the same as those used in the two-stage nozzle (reference 1). Further discussion as to the accuracy of the pressure recording instruments is desirable herein, however, because of the lower range of operating pressures.

The maximum error of the pressure cells can be held to 0.01 inch of deflection with careful calibration and use. Full-scale deflection from all cells is approximately 2 inches; therefore, the accuracy of any particular reading depends on the range of the cell used and the pressure measured. The lowest range and hence the most accurate low-pressure cell available at this time is one with a range of 0 to 0.8 inch of mercury. This type of cell is accurate to 2 percent at the range of static pressures normally encountered in the test section. More accurate instruments cannot be used because of the short durations of the runs and the variations in flow conditions with time.

METHODS AND PROCEDURES

Wall pressures.- Wall pressures along the nozzle are obtained from 0.025-inch-diameter orifices in the side-wall plates. Standard $\frac{1}{4}$-inch brass fittings and copper or neoprene tubing are used to transmit the wall pressures to the instruments.

Stream static pressures.- Stream static pressures are measured with "needle" probes. The probe consists of a cone-cylinder body 1/8 inch in diameter with four pressure orifices 0.025 inch in diameter drilled 90° apart around the periphery of the cylinder. In order to determine the best probe proportions, an investigation was made of the effect of orifice location and cone angle on the pressures measured. Theoretical calculations at a Mach number of 6.75 and for an included cone angle of 20° showed that the surface pressure on the cylinder was 93 percent of stream pressure at 16 diameters from the apex of the cone. Experimental results showed that with an included cone angle of 10° no measurable difference in surface pressure could be obtained from 8 to 40 diameters from the apex. Variation of the cone angle from 10° to 40° produced no change in pressure at 16 diameters from the apex. However, the measured pressure was sensitive to the distance of the orifices from the probe support strut. Satisfactory results were obtained with the orifices located a minimum of 16 diameters from the support strut.

The tests indicated that a probe with an orifice location of 16 diameters from the apex and 30 diameters from the strut and an included cone angle of 10° will measure stream static pressures within the accuracy of the pressure instruments. These probe proportions were used on the static survey rake illustrated in figure 3. The leadout tubes to the pressure cells are about 3 feet long and have an inside diameter of 1/8 inch.

The time response of this system is less than 10 seconds for a change in pressure from 2 inches of mercury to within 2 percent of a final constant value of 0.2 inch of mercury. The effect of lag was minimized by evacuating the nozzle and pressure instruments to less than 2 inches of mercury before a run.

The center-line survey of the stream static pressures was made with a single-needle probe. The needle itself is about $1\frac{1}{2}$ times larger than but has approximately the same proportions as those on the static rake.

Impact pressures.- The impact-pressure surveys were made with a rake similar to the static-pressure rake in figure 3. The static tubes shown, however, were cut off square 3/4 inch from the leading edge of the rake to form impact-pressure tubes. The diameter of the opening in the end of the tubes is one-half the outside diameter of the tubes.

Stagnation temperature.- The stagnation-temperature surveys were made with the temperature probe described in reference 1. Although the temperature measured by this probe may be as much as 2 percent lower than the true stagnation temperature, comparative values in a survey should be much more accurate.

Flow angles.- A 10° wedge of 9-inch span and 2-inch chord was used to measure flow angles. The wedge has seven pairs of opposing orifices 1 inch from the leading edge and 1 inch apart. The difference in pressure across the opposing orifices and the local Mach number from the static- and impact-pressure surveys were then used to calculate the local flow angle.

OPERATING CONDITIONS

For the purpose of making calibration surveys of the nozzle certain operating conditions are held to close limits. The settling-chamber temperature is maintained above 1100° R to avoid the possibility of liquefaction of the air in the test section. The maximum dew point is 400° R at a pressure of 1 atmosphere. Progressive changes in flow parameters have been found to occur if both of these conditions were not satisfied.

The stagnation conditions for a typical run are shown in figure 4. The settling-chamber pressure p_o is held constant by the pressure regulating valve after the first 5 seconds of running time. The settling-chamber temperature T_o is essentially constant for the last 30 seconds of the run. This figure also shows the variation with time of the stream static and impact pressures in the test section.

The test Reynolds number per foot of length is relatively high because of the high velocity and the low viscosity. At the test section the Reynolds number per foot is about 3×10^6 for a stagnation pressure of 25 atmospheres.

RESULTS AND DISCUSSION

Variation of flow properties with time.- The results of a typical run show that the stream static and impact pressures in the test section decrease with time. This effect was present in all stream pressure data obtained and in most of the wall static-pressure data ahead of the test section.

The pressure changes indicate about a 3-percent increase in stream Mach number during the time interval from 10 to 60 seconds. The pressures measured in the portion of the run from 0 to 10 seconds must be largely ignored because of the rapidly changing conditions and because of instrument lag.

The changing flow conditions in the stream can be accounted for by an inward movement of the effective boundary at the throat. Because of the slitlike configuration of the throat a small change in its dimensions results in a relatively large percentage change in its area. Thus an inward movement of both the top and bottom effective boundaries of about 0.006 inch changes the effective one-dimensional area ratio enough to increase the Mach number by 3 percent.

Measurements show that the nozzle blocks have taken a permanent set in the region of the throat. The largest deflection is in the center of the blocks such that the throat opening is somewhat oval-shaped with an average increase in the Z-ordinate of 0.004 inch. The large stresses necessary to cause this permanent set probably originated from the nonuniform heating of the blocks during a run. Since these temperature stresses are of sufficient magnitude to cause a permanent set, it seemed reasonable to expect measurable deflections during a run. Accordingly, several dial indicators were set up along a line parallel to the Y-axis at $X = 0$. The indicators were arranged to bear at points about 1/2 inch from the inside surface of the nozzle contour as shown in figure 2. Three indicators were located at the top and three at the bottom of the nozzle. In order to show any relative change in the throat opening, all six indicators were mounted on the same frame which was suspended from a single point at the top of the nozzle. At a stagnation temperature of 1150° R, the measurements showed that both the top and bottom surfaces were warping inward at the rate of about 0.001 inch every 10 seconds at $Y = 0$. At the side walls the deflection decreased to essentially zero. At 60 seconds the Z-ordinate in the throat at $Y = 0$ was about 0.002 inch less than the design value of 0.0479 inch. During the time interval from 10 to 60 seconds the throat area thus decreased from approximately 0.508 to 0.461 square inch. Within the accuracy of the data, this change is sufficient to account fully for the increase in Mach number with time observed in the test section. At a stagnation temperature of 530° R no measurable deflection was obtained and the pressures in the test section were constant throughout the run (except for lag effects).

Another possible contributing factor for a part of the Mach number variation with time is an increase in boundary-layer displacement thickness δ^* as the inside surfaces of the nozzle blocks become heated during a run. Estimates based on simplified methods of boundary-layer calculation with no heat transfer indicated, however, that the boundary layer in the throat was so thin that even if it were decreased by 100 percent the change in the effective throat area would be small compared with the changes caused by warpage of the nozzle blocks.

Variation of flow parameters with settling-chamber pressure.- Stream pressure surveys were made at (55.8,0,Z) through a range of settling-chamber pressures from 25 to 3 atmospheres. The stagnation temperature was maintained above 1110° R. The averages of the pressure ratios at several vertical stations are plotted in figure 5 as functions of p_o. The Mach number as obtained from p_1/p_t is also plotted. The figure shows that the change in the static- and impact-pressure ratios is such that the Mach number is almost constant down to a value of p_o of 12 atmospheres. Below 12 atmospheres the pressure ratios increase more rapidly and indicate that the Mach number decreases to about 6.2 at $p_o = 3$ atmospheres. The exact decrease in the Mach number is not certain because of the difficulty of obtaining accurate measurements of the static pressure over the lower range of settling-chamber pressure. Measurements of shock angles from the static probes, however, result in a Mach number decrease of about the same magnitude as obtained from pressure data. It is thus fairly certain that the average stream Mach number at $p_o = 3$ atmospheres is between 6.00 and 6.40. Comparison of these values with the isentropic Mach number from the impact-pressure data, for example, shows that a total-pressure loss of about 20 percent occurs for the initial stagnation pressure of 3 atmospheres. A possible cause for this total-pressure loss is a series of compression waves which appear to exist at the low pressures. The presence of these waves was indicated by the type of static-pressure distribution obtained at low densities. The impact-pressure distributions showed that the boundary layer in the test section had not thickened appreciably at the low densities. For these reasons the viscous effects in the center of the stream are probably not the main cause of the loss in total pressure. Some reduction in heat transfer to the nozzle blocks should be expected to result from the lower density. This reduction would cause only a very small decrease in Mach number as compared with the change that occurs from 12 to 3 atmospheres.

Calibration surveys.- In order to determine the flow characteristics in the nozzle, stagnation conditions were maintained at about 25 atmospheres and approximately 1200° R. The dew point at atmospheric pressure was less than 400° R. All data presented were taken 60 seconds from the beginning of the runs in order to minimize the effect of nozzle warpage with time. The warpage of the first minimum during the heated runs is, of course, affected by several factors such as the stagnation temperature, the initial temperature of the nozzle blocks, stagnation pressure, and even the variation of the temperature and pressure with time. In general, for the calibration runs, these conditions do not vary greatly so that their individual effects are small; however, scatter in the data results. The first several runs made with the nozzle have not been used because of difficulty in repeating the data. The nozzle was probably acquiring the permanent set in the throat region during these first runs, and therefore progressive changes in the flow occurred.

Static pressures were measured at a large number of points on the parallel walls of the nozzle. The results of this survey are presented as pressure contour lines in the lower half of figure 6. For comparison the theoretical contours are shown in the upper half of the figure. The orifice locations are indicated by small crosses.

The actual contour lines upstream from the region of $\frac{p_w}{p_o} = 3 \times 10^{-4}$ are in good agreement with the theoretical contours. Downstream from this region the flow deviates from the theoretical flow. However, the gradients are relatively small in this region and the contour plot overemphasizes the deviations. Since boundary layer was ignored in the nozzle design, the flow is not expected to conform exactly to the potential flow. Downstream from $X = 45$ the gradients may be influenced slightly by small leaks in the walls of the nozzle. These leaks had no effect in the central portion of the stream in the region of the test section because of the small Mach angles of the flow.

The Mach number along the center line of the parallel walls was determined from p_w/p_o for $\gamma = 1.400$. The resulting Mach number distribution is plotted in figure 7, which includes the theoretical distribution. The Mach number decreases as the test section is approached and is always lower than the maximum theoretical Mach number.

Static and impact pressures were measured along a part of the longitudinal axis of the nozzle. This survey extended from the center of the test section (55.8,0,0) to a point about 16 inches upstream. The data are presented in figure 8 as the ratio of local pressure to settling-chamber pressure. Comparison of the Mach number distributions as obtained from p_1/p_o and p_t/p_o shows close agreement. This agreement indicates that the flow along the axis is nearly isentropic; however, the wavy distribution indicates that a series of weak compression and expansion waves are present along the center line.

Complete surveys were made of the static and impact pressures in the plane perpendicular to the longitudinal axis of the nozzle at $X = 55.8$. The results of the horizontal surveys at $Z = 1$, -1, and 0 are shown in figure 9. The results of the vertical surveys at $Y = 2$, 0, and -2 are shown in figure 10. The faired curves represent averages of a large number of runs.

Most of the static-pressure data show an appreciable amount of scatter. Since the static pressure is very low (about 0.2 in. Hg), about 3-percent error is due to instrumentation difficulties and measuring technique. Much of the remaining scatter is due to the sensitivity of the flow to small changes in the boundaries at the narrow slitlike throat. Factors that cause these changes have been discussed previously.

The impact-pressure distributions in figure 9 indicate the presence of a boundary-layer development which seems to be characteristic of two-dimensional nozzles. This type of boundary-layer development is the low-velocity region that extends farther into the flow along the center line of the side plates than on either side of the center line. The same type of boundary-layer development was encountered in the first expansion of the two-stage nozzle (reference 1).

The Mach number distributions in the test section are presented in figures 11 and 12 as calculated from the ratios p_1/p_o, p_t/p_o, and p_1/p_t. The last ratio involves only local measurements and its use to determine the Mach number does not require any assumptions regarding the character of the flow in the nozzle. However, at high Mach numbers the function $M(p_1,p_t)$ is extremely sensitive to small changes in the ratio p_1/p_t. For this reason, if the flow is isentropic, the values of M as obtained from p_1/p_o and p_t/p_o may be more reliable. The Mach number curves of figures 11 and 12 were computed from the faired pressure curves (figs. 9 and 10). The Mach number distribution is reasonably uniform in a region 6 inches high by 5 inches wide centered on the axis of the tunnel. The average Mach number in this region is about 6.86. The good agreement between $M(p_1,p_o)$ and $M(p_t,p_o)$ in this central region indicates that the flow is very nearly isentropic.

Flow-angle surveys were made in the YZ plane at $X = 55.8$. The pressure differences across the opposite surfaces of a 10° wedge together with the local Mach numbers from figures 11 and 12 were used to compute the flow angles from the oblique-shock equations. Typical results are shown in figure 13, in which a positive value of ϵ_h is taken as the horizontal flow deflection in the direction of increasing Y and a positive value of ϵ_v is the vertical flow deflection in the direction of increasing Z. Figure 13(b) indicates that the flow diverges slightly in the vertical direction from the tunnel axis. This divergence is less than 0.3° within a region nearly 5 inches square in the center of the test section. Figure 13(a) shows a slight convergence toward the center at $Z = 0$ and a slight divergence 2 inches above and below this station. In figure 13(b) the curves at $Y = 0$ and $Y = 2$ appear to be asymmetrical in regard to the line of $\epsilon_v = 0$. This effect is due primarily to inaccuracies in construction of the wedge. These inaccuracies and the errors in setting the angle of attack resulted in a maximum error of about 0.2° in the flow-angle data.

Stagnation-temperature surveys were made in the YZ plane at $X = 55.8$. The results of these surveys are presented in figure 14 as the ratios of the absolute stagnation temperature to the absolute settling-chamber temperature. The figure indicates that an approximately constant temperature recovery of 98 percent or better exists in a region which corresponds

roughly to the region of constant static and impact pressures. The sharp peaks in the curves of T_o'/T_o for the horizontal center plane ($Z = 0$) are apparently caused by the large amount of heat conducted toward the free stream as a result of the large static-temperature gradients between $Y = 2.75$ and 3.5 at $Z = 0$.

General discussion of the nozzle characteristics and correlation of the data.- The center-line distribution of impact pressures (fig. 8) and the assumption of zero flow angle along the center line were used to construct a characteristics net in a portion of the nozzle (fig. 15). The net was extended to (55.8,0,Z) by assuming that any additional disturbance from the wall would not change the flow, as indicated in figure 15. The results of the calculation are in agreement with the impact-pressure and flow-angle data at (55.8,0,Z) within the scatter of the data. Since the assumptions in regard to two-dimensional flow may not be strictly correct and since the accuracy and extent of the data are limited, the agreement obtained by this method may be subject to qualification.

Boundary-layer growth along the nozzle contour was calculated by using a $\frac{1}{7}$-power velocity profile and the density and kinematic viscosity at the wall to evaluate the local skin-friction coefficient. The pressure gradient based on the potential flow was used. These calculations resulted in a value for δ^* of about 0.6 inch at $X = 55.8$. Integration of the survey data gave an actual value of δ^* between 0.70 and 0.75 inch, depending on the temperature profile assumed. The calculation also indicated that the boundary-layer growth is approximately linear at an average angle of 0.7° with respect to the surface.

The results from stream static- and impact-pressure surveys along the axis of the nozzle indicate the presence of a series of compression and expansion waves. The effects of these waves are difficult to measure in the YZ plane because of the small Mach angles. The total-pressure loss and effect of the waves on the flow are negligibly small at normal operating pressures. As the settling-chamber pressure is decreased, a loss in total pressure as indicated by the magnitude of the decrease in Mach number is noted.

At normal operating pressures the nozzle produces an isentropic-flow region 6 inches high by 5 inches wide where the maximum variation from the average Mach number of 6.86 is about 1 percent. The angular deviations from parallel flow in this region are less than 1° and in a region nearly 5 inches square flow angles were less than 0.3°. Studies indicated that the flow was sensitive to changes in the boundary at the slitlike throat.

Comparison of the results from the single-stage nozzle with those from the two-stage nozzle (reference 1) shows that the single-stage

nozzle is far superior in all respects except in the variation of Mach number with time. The two-stage nozzle with its nearly square first minimum did not suffer from first-minimum boundary change with heating of the nozzle blocks and consequently had no variation of Mach number with time. The more uniform flow and flow angles on the order of 1/10 of those in the two-stage nozzle make the single-stage nozzle more suitable for use at this Mach number.

Significant improvement of the flow in this nozzle could probably be obtained by correcting the nozzle contour for boundary layer. Refinements of this nature are not warranted, however, until the more pronounced warpage effects have been eliminated.

CONCLUDING REMARKS

Flow surveys made in the Langley 11-inch hypersonic tunnel have shown that a single-expansion nozzle produces reasonably uniform flow with an average free-stream Mach number of 6.86. The nozzle was designed for a Mach number of 7.08 by the method of characteristics with no boundary-layer corrections. Calibration surveys were made at a stagnation pressure of 25 atmospheres and a stagnation temperature of 1210° R. Isentropic flow was obtained at the test section in a region approximately 6 inches high by 5 inches wide where the maximum deviation from the average Mach number was about 1 percent. The angular flow deflections in this region were less than 1°, and in a region nearly 5 inches square the flow deflections were less than 0.3°.

The test-section Mach number was found to increase about 3 percent from the beginning to the end of a 60-second test run. This variation was found to be caused primarily by warpage of the nozzle blocks near the throat of the nozzle due to large temperature gradients.

Decreasing the settling-chamber pressure had no appreciable effect on the Mach number distributions until the pressure was decreased below 12 atmospheres. Below 12 atmospheres the Mach number decreased rapidly with decreasing settling-chamber pressure.

Langley Aeronautical Laboratory
National Advisory Committee for Aeronautics
Langley Field, Va., September 25, 1950

REFERENCE

1. McLellan, Charles H., Williams, Thomas W., and Bertram, Mitchel H.: Investigation of a Two-Step Nozzle in the Langley 11-Inch Hypersonic Tunnel. NACA TN 2171, 1950.

TABLE I

NOZZLE DESIGN COORDINATES

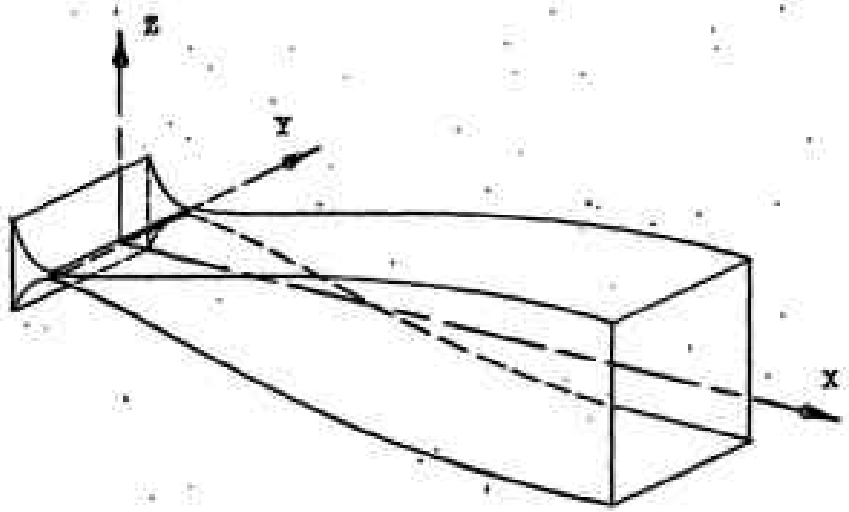

Approach section		Expansion	
X (in.)	Z (in.)	X (in.)	Z (in.)
-1.781	2.000	0	0.0479
-1.656	1.806	.048	.0487
-1.531	1.613	.096	.0512
-1.281	1.227	.144	.0554
-1.031	.858	.191	.0613
-.781	.520	.239	.0689
-.731	.457	.287	.0782
-.681	.395	.335	.0892
-.631	.338	.383	.1021
-.581	.284	.431	.1167
-.531	.233	.479	.1332
-.481	.188	.527	.1516
-.431	.150	.574	.1719
-.381	.123	.622	.1942
-.356	.112	.670	.2186
-.331	.102	.800	.2915
-.306	.092	1.012	.4066
-.281	.084	1.304	.5504
-.256	.0753	1.742	.7485
-.231	.0700	2.239	.9549
-.206	.0650	2.876	1.190
-.181	.0600	3.707	1.467
-.156	.0550	4.798	1.787
-.131	.0540	6.327	2.178
-.106	.0520	8.280	2.607
-.081	.0500	10.925	3.089
-.031	.0480	14.651	3.635
-.016	.0479	19.792	4.207
		26.862	4.744
		35.973	5.125
		46.022	5.257

NACA

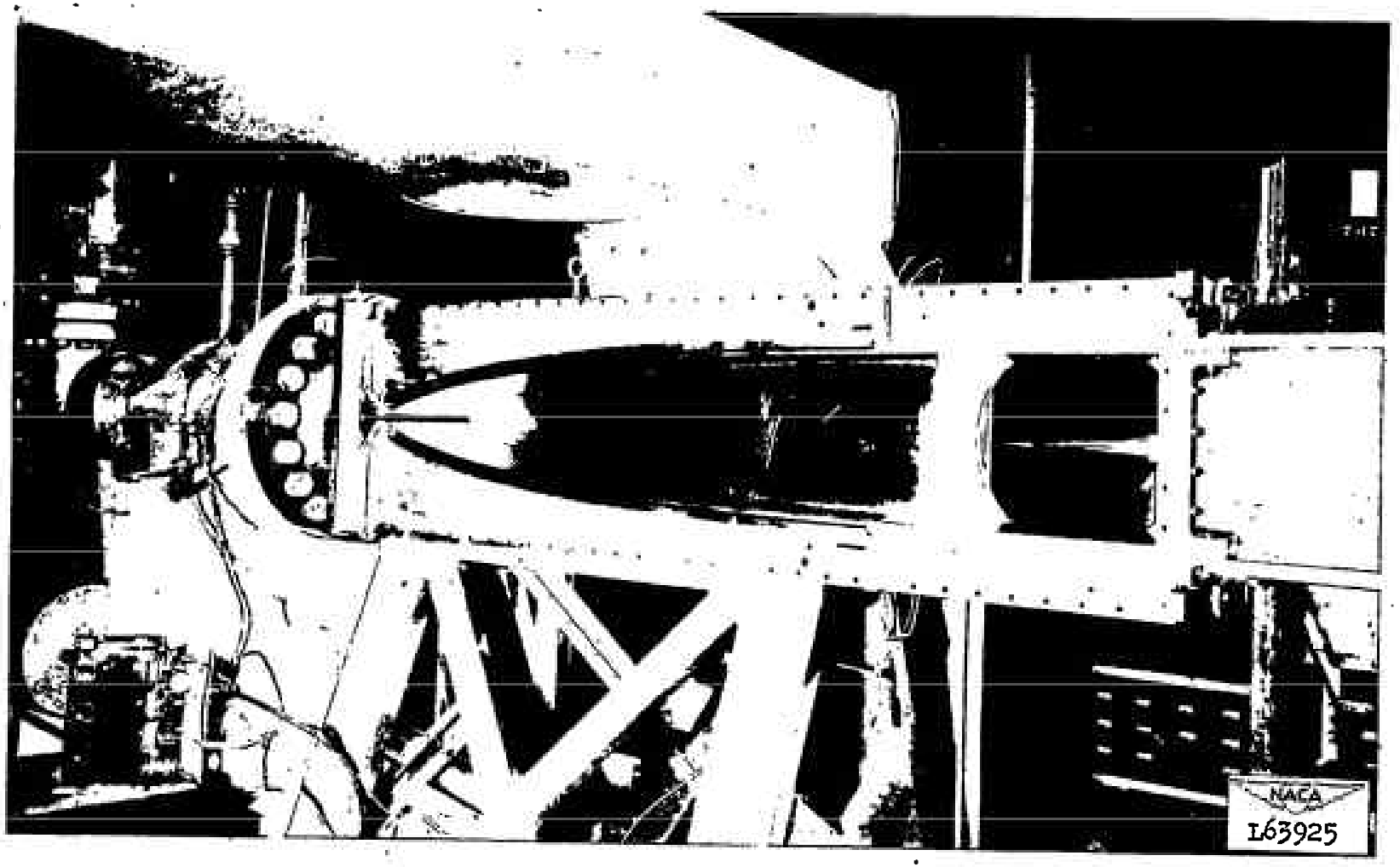

Figure 1.- View of the nozzle with side plate removed with the wedge survey probe shown mounted in the test section.

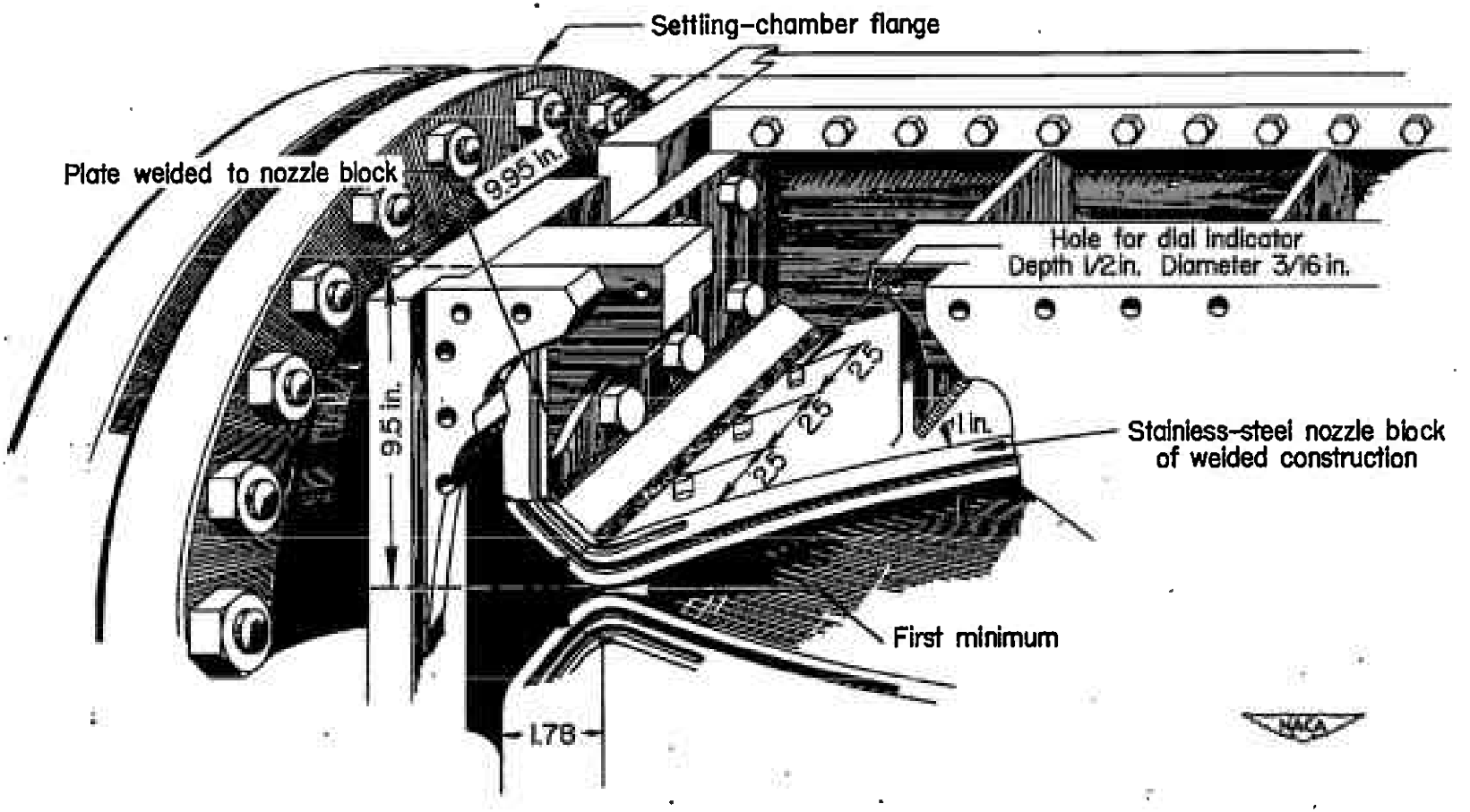

Figure 2.- Cutaway view of a part of the nozzle with the type of construction shown.

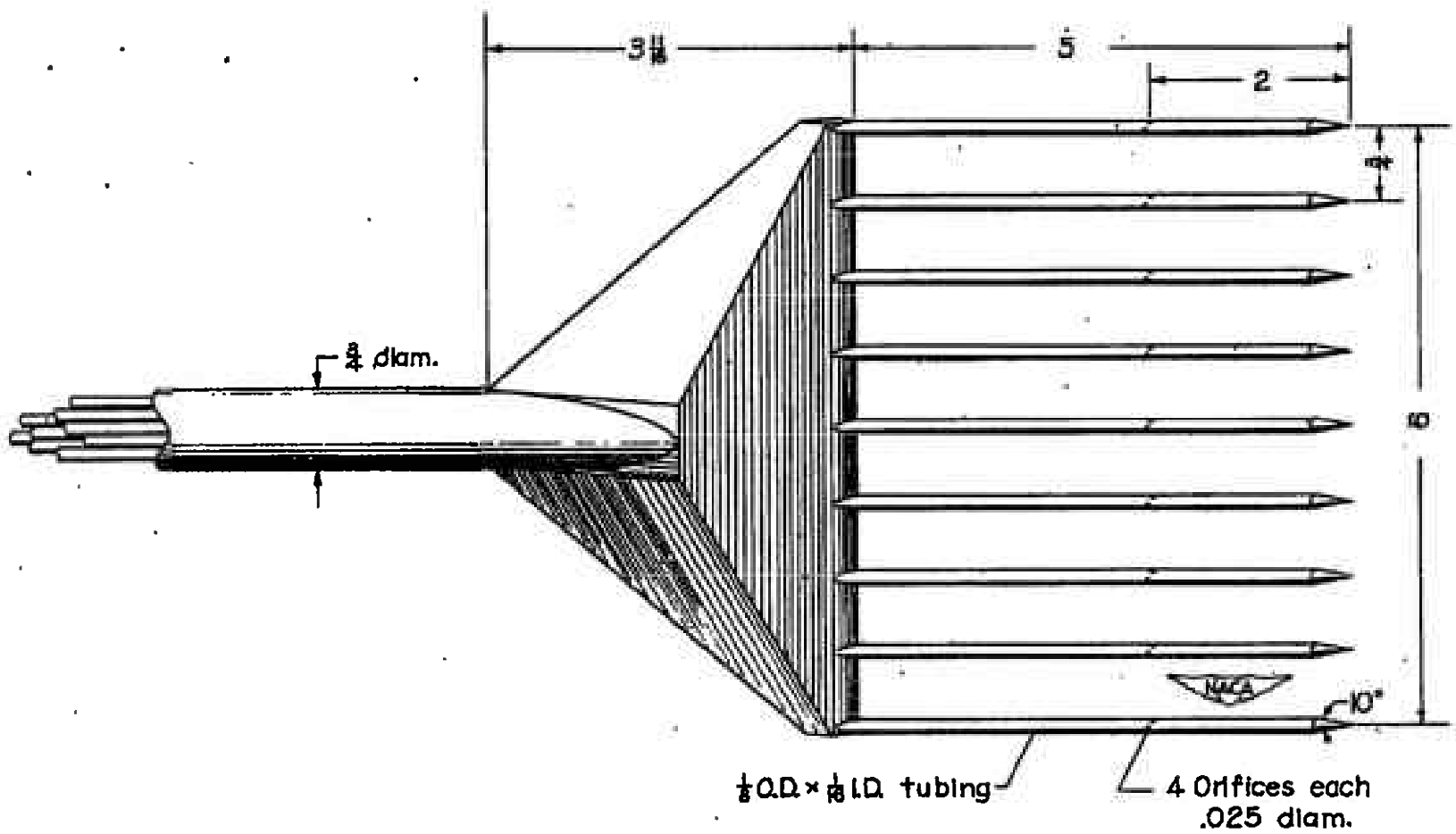

Figure 3.- Stream static-pressure rake. All dimensions are in inches.

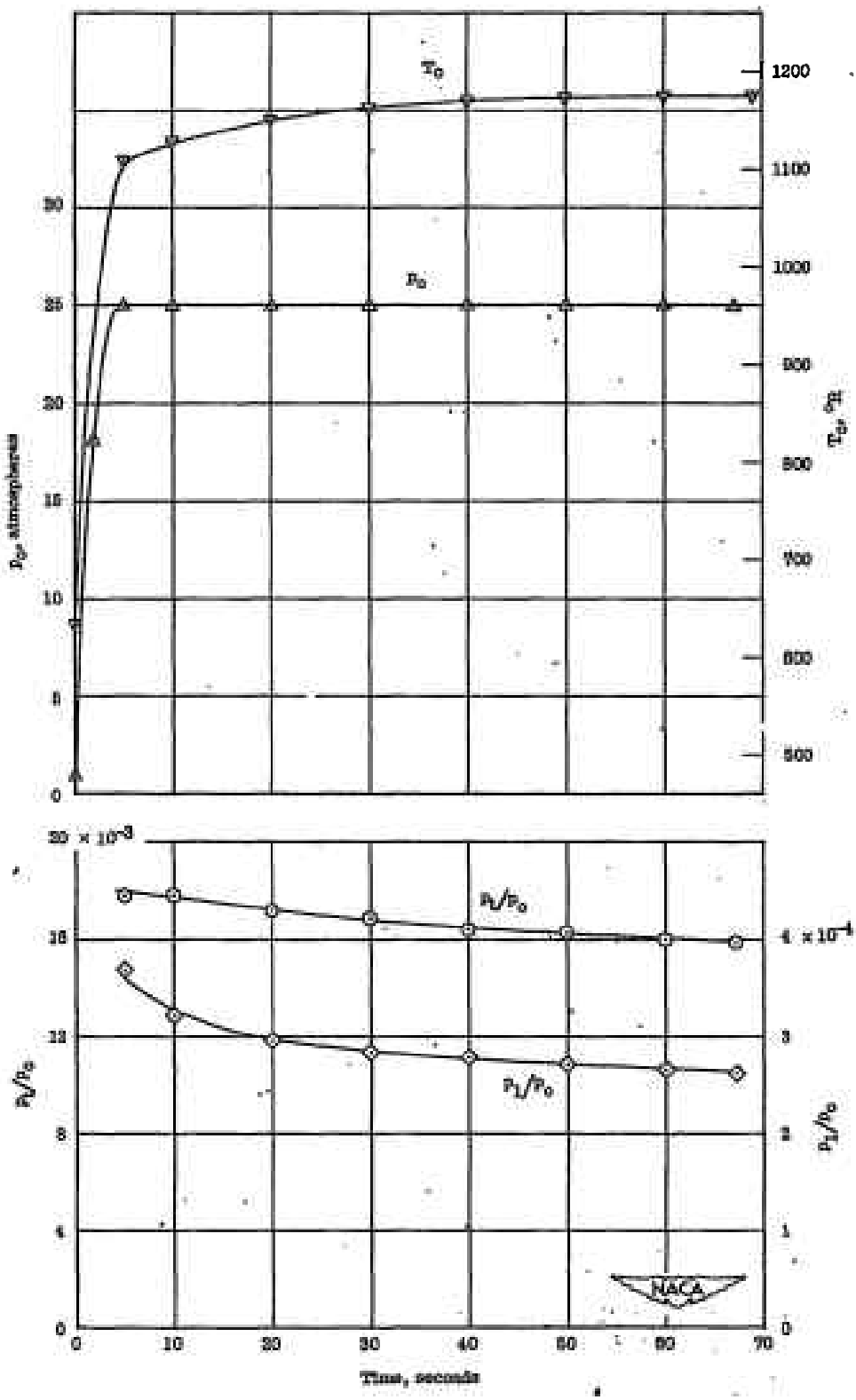

Figure 4.- Results from a typical test on the nozzle.

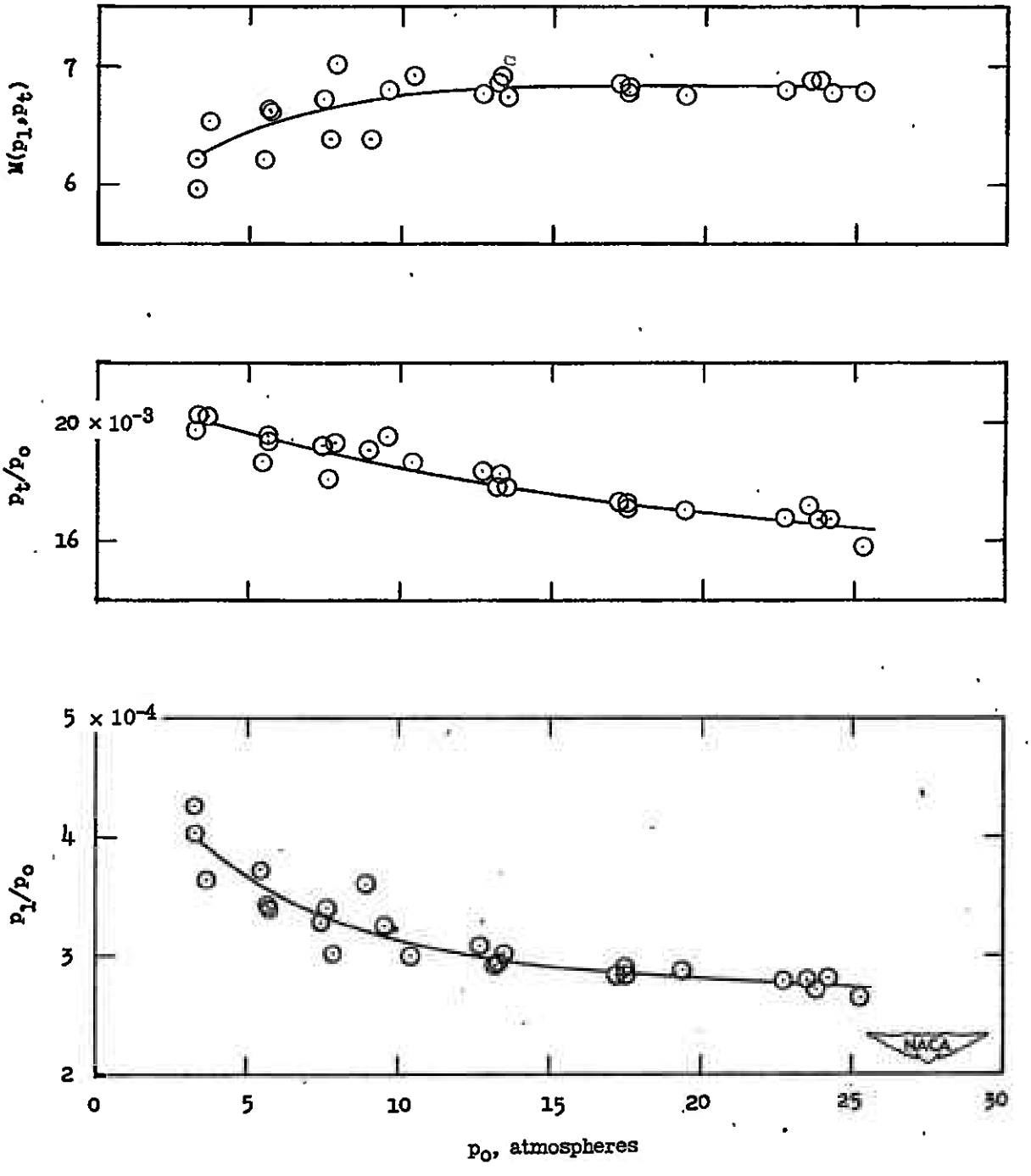

Figure 5.- The average variation of static- and impact-pressure ratios and Mach number with settling-chamber pressure at X = 55.8, Y = 0, and Z = -3 to 3.

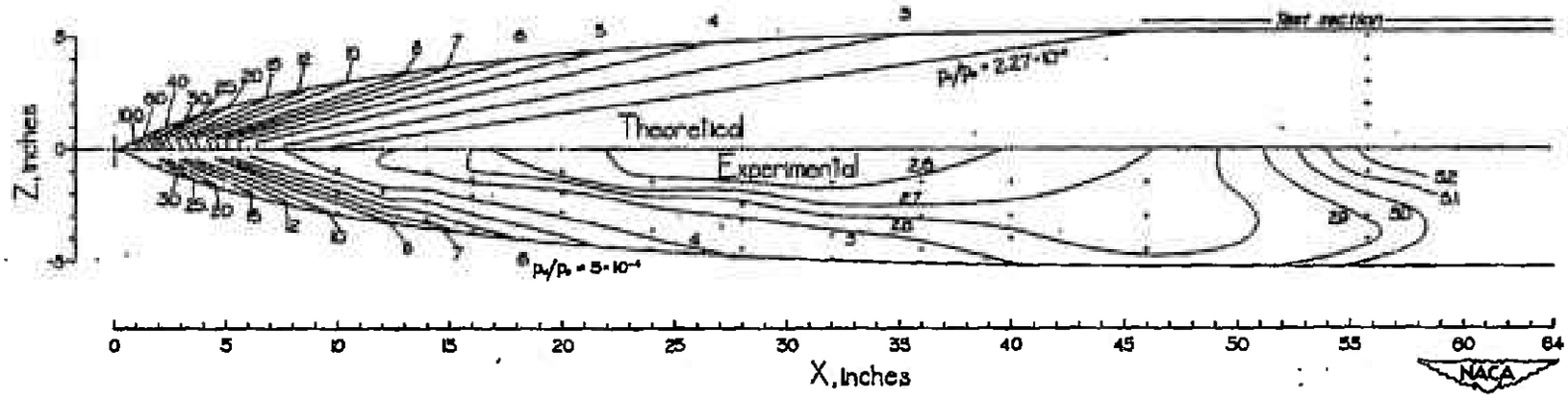

Figure 6.- Pressure contours on the side plate of the nozzle.

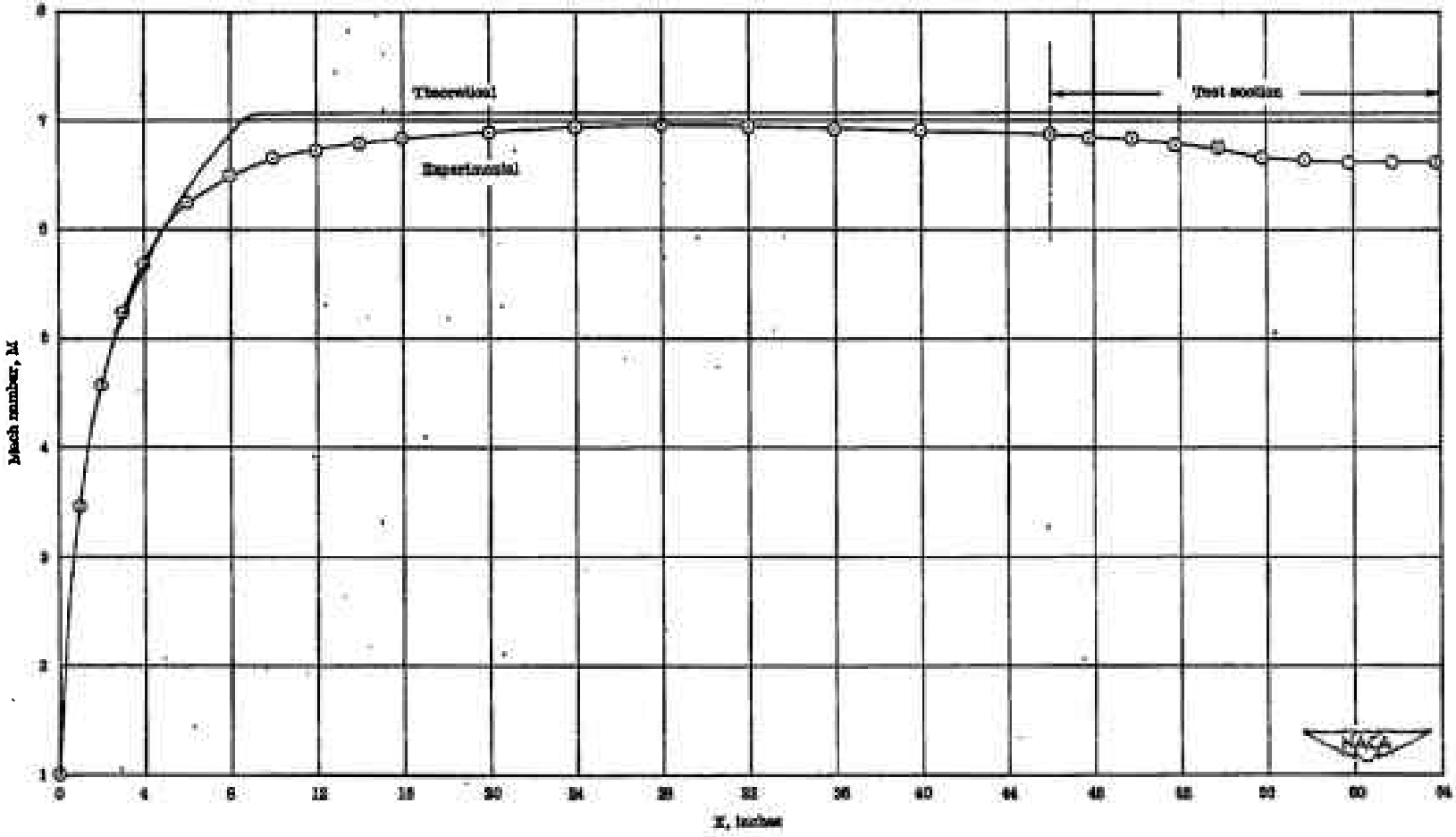

Figure 7.- Mach number distribution from static pressures along the center line of the side plate.

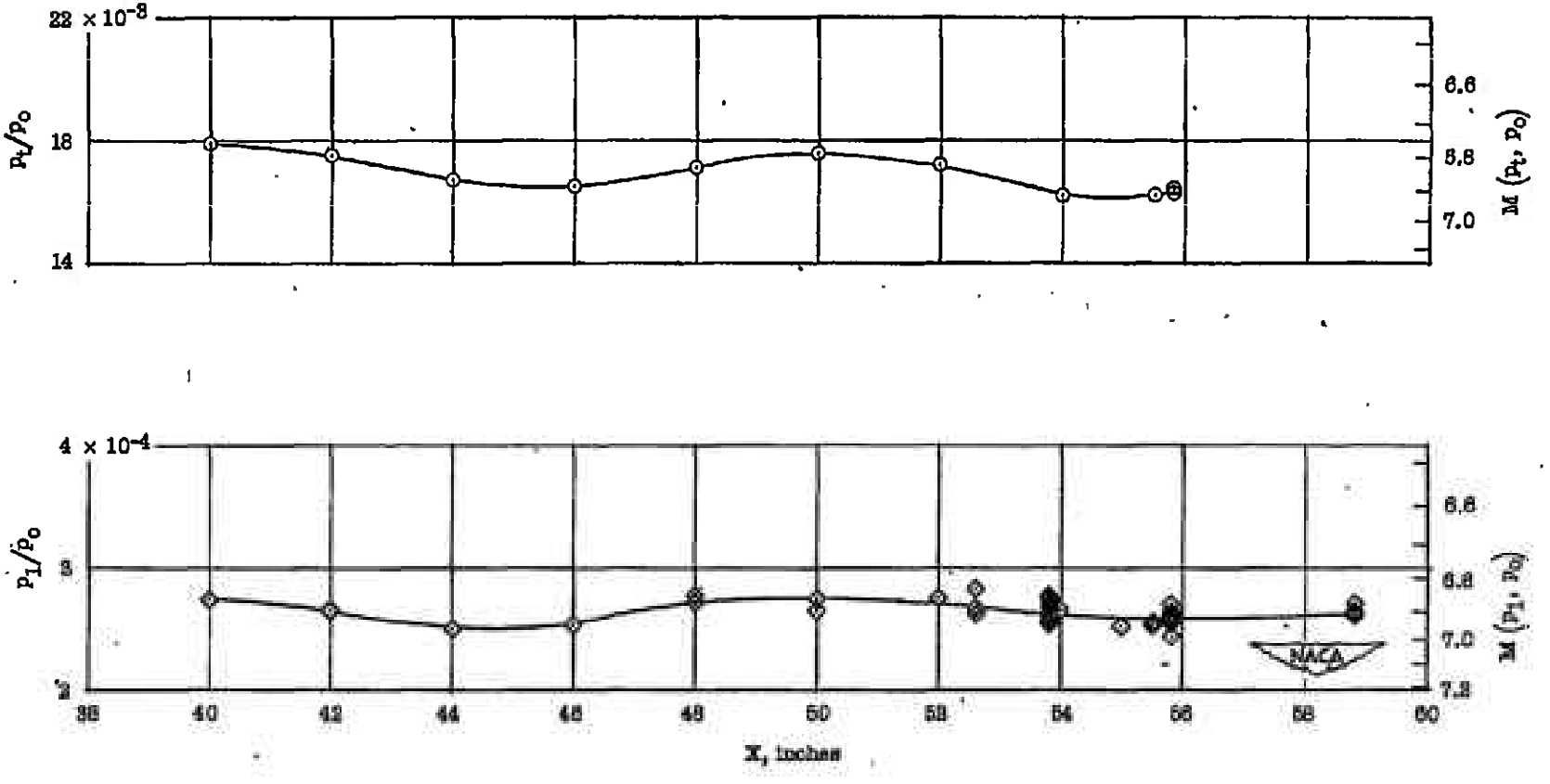

Figure 8.- The distribution of stream static- and impact-pressure ratios along the X-axis.

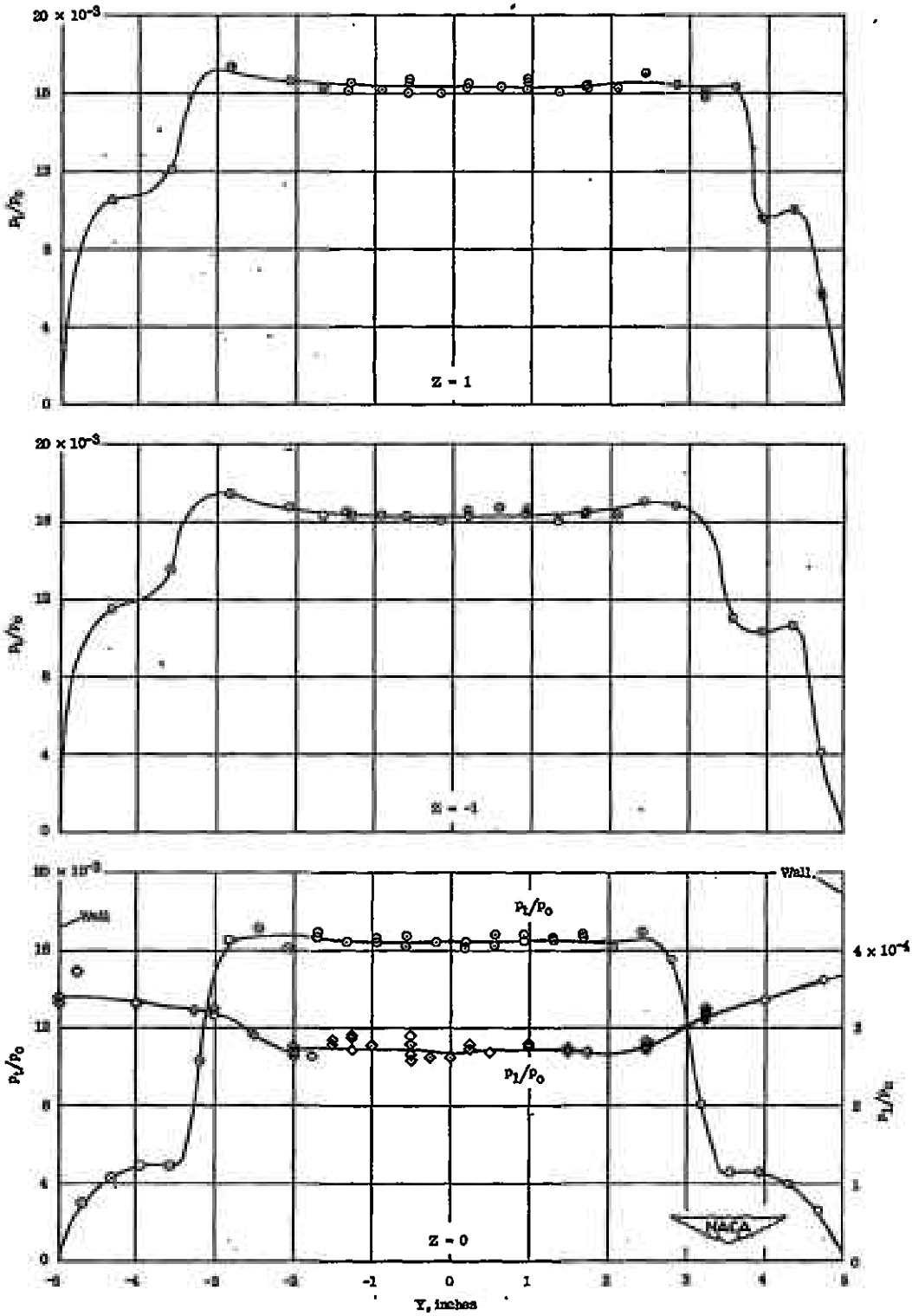

Figure 9.- Static- and impact-pressure ratios plotted against horizontal station at X = 55.8 and Z = 1, -1, and 0.

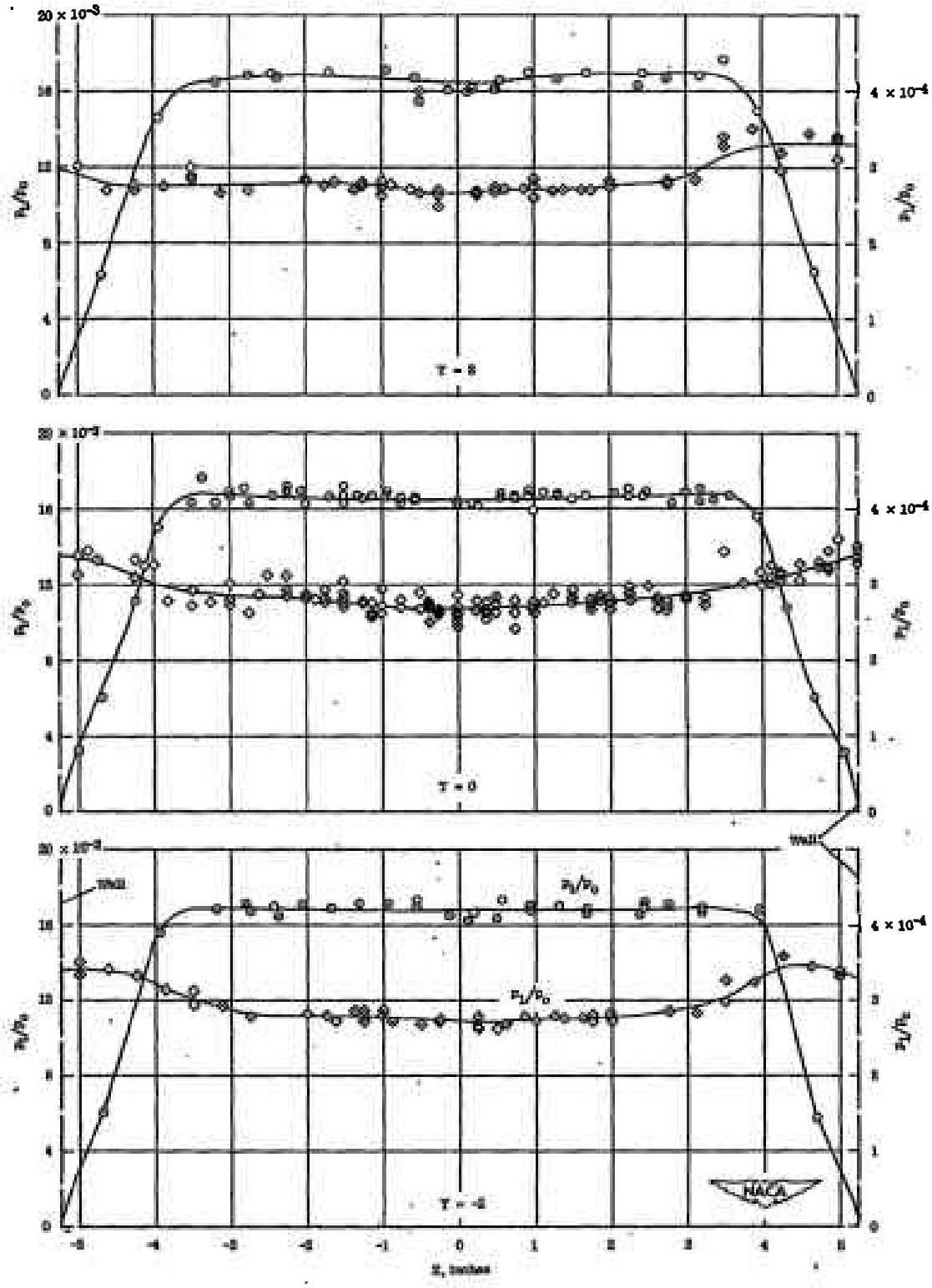

Figure 10.- Static- and impact-pressure ratios plotted against vertical station at X = 55.8 and Y = 2, 0, and -2.

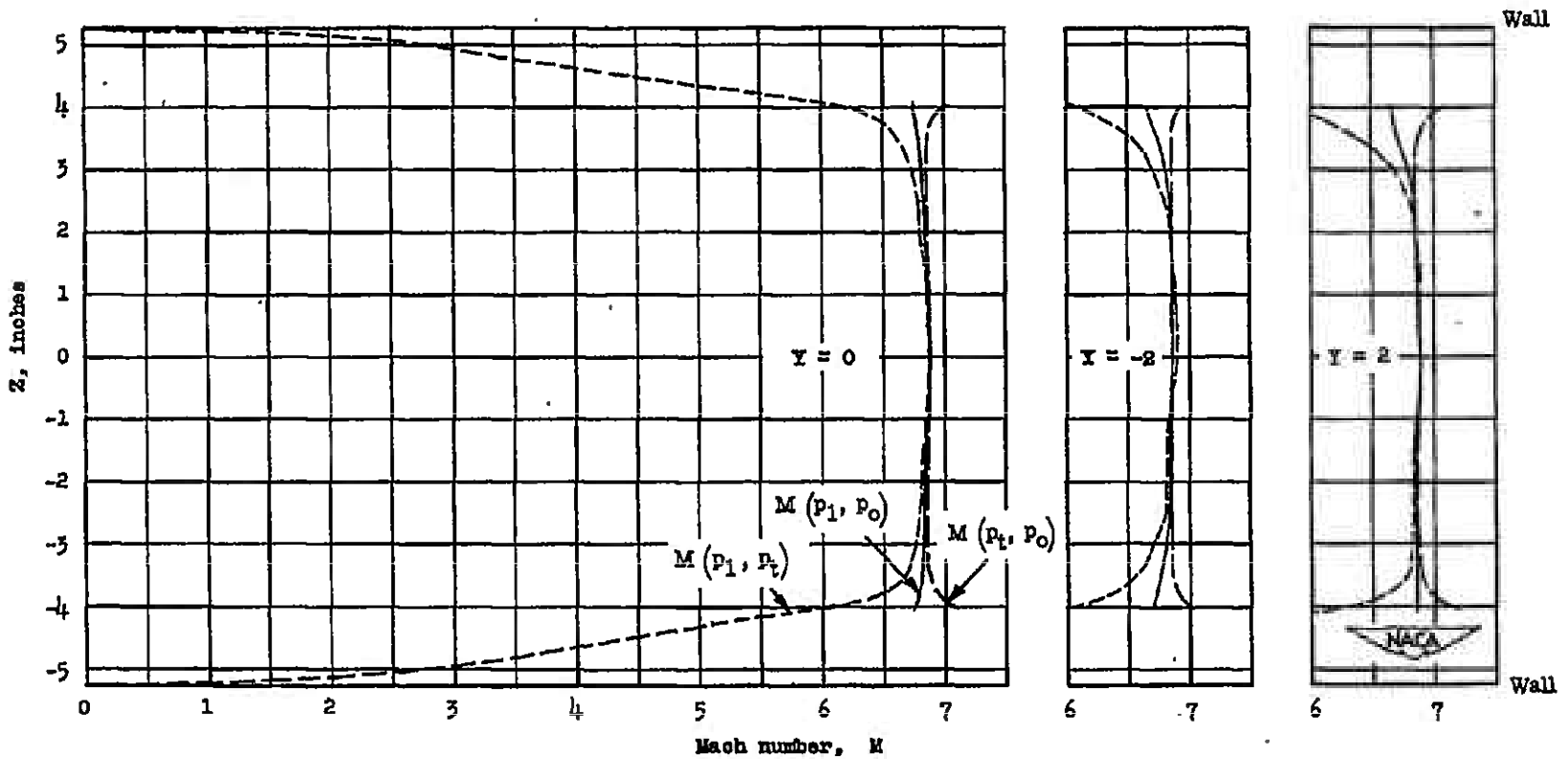

Figure 11.- Mach number plotted against vertical station at X = 55.8 and Y = 0, -2, and 2.

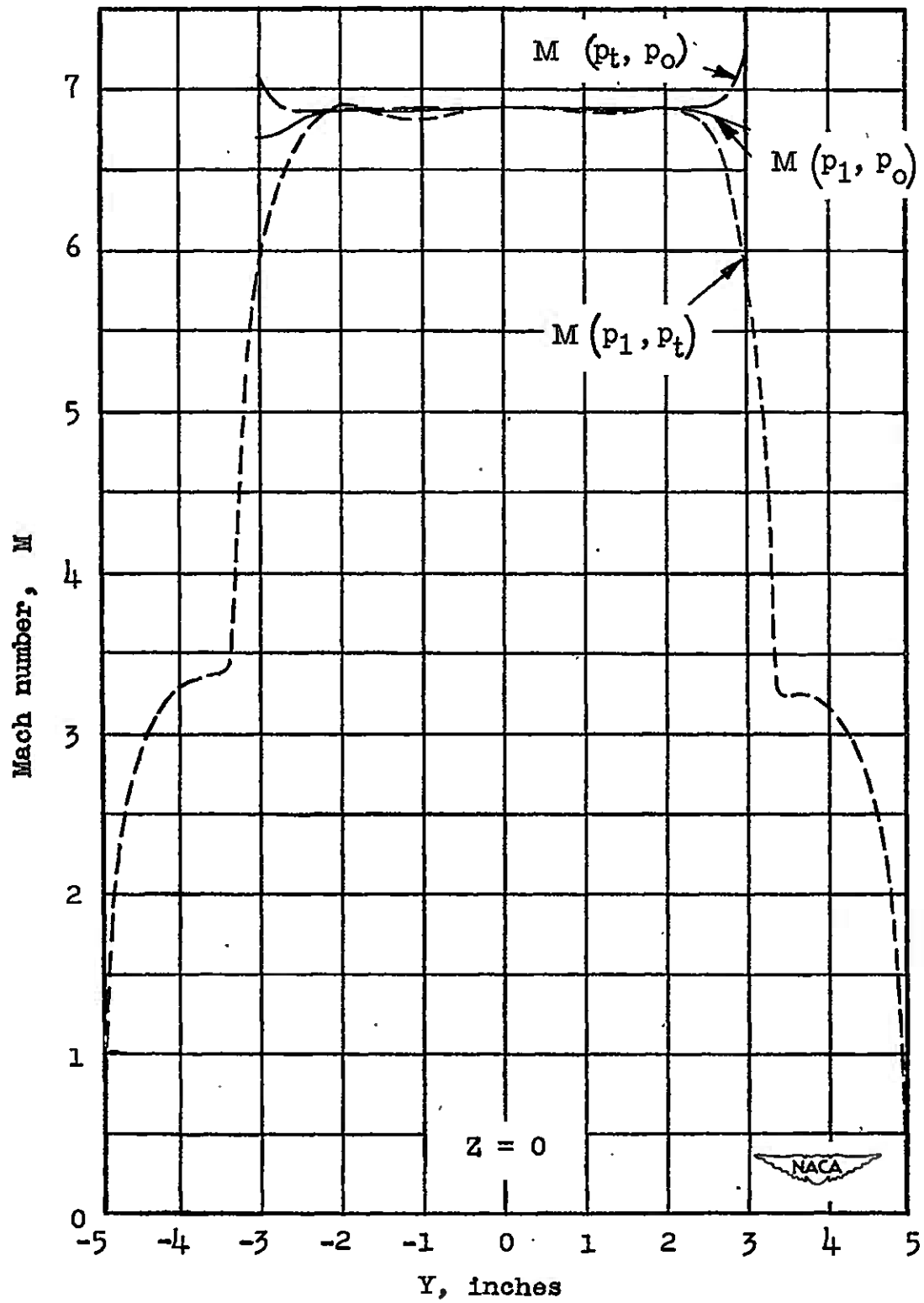

Figure 12.- Mach number plotted against horizontal station at X = 55.8 and Z = 0.

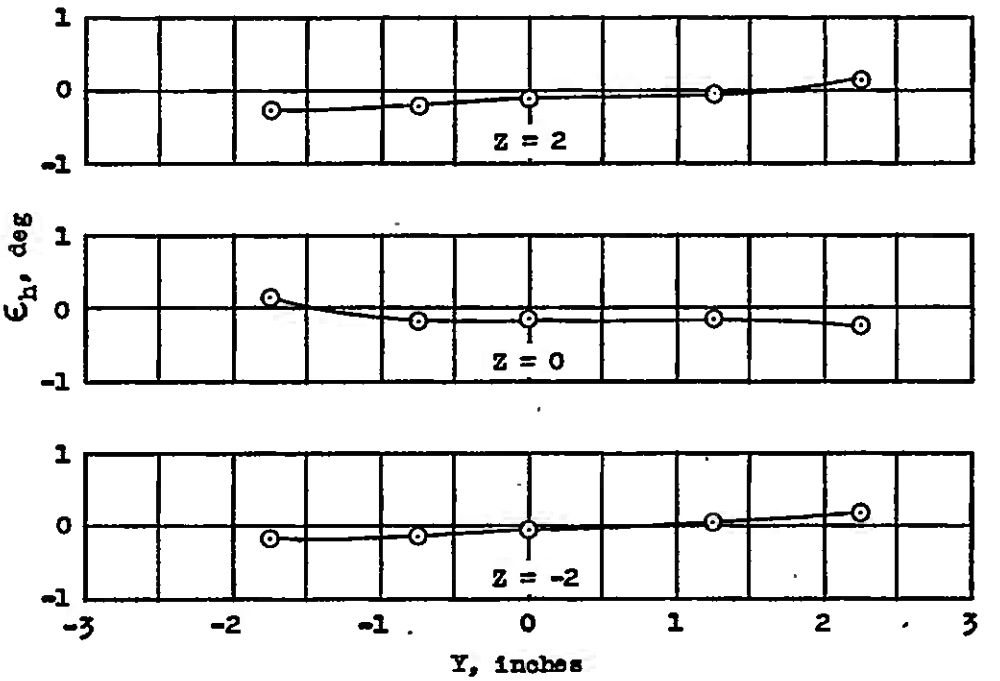

(a) Flow angle plotted against horizontal station.

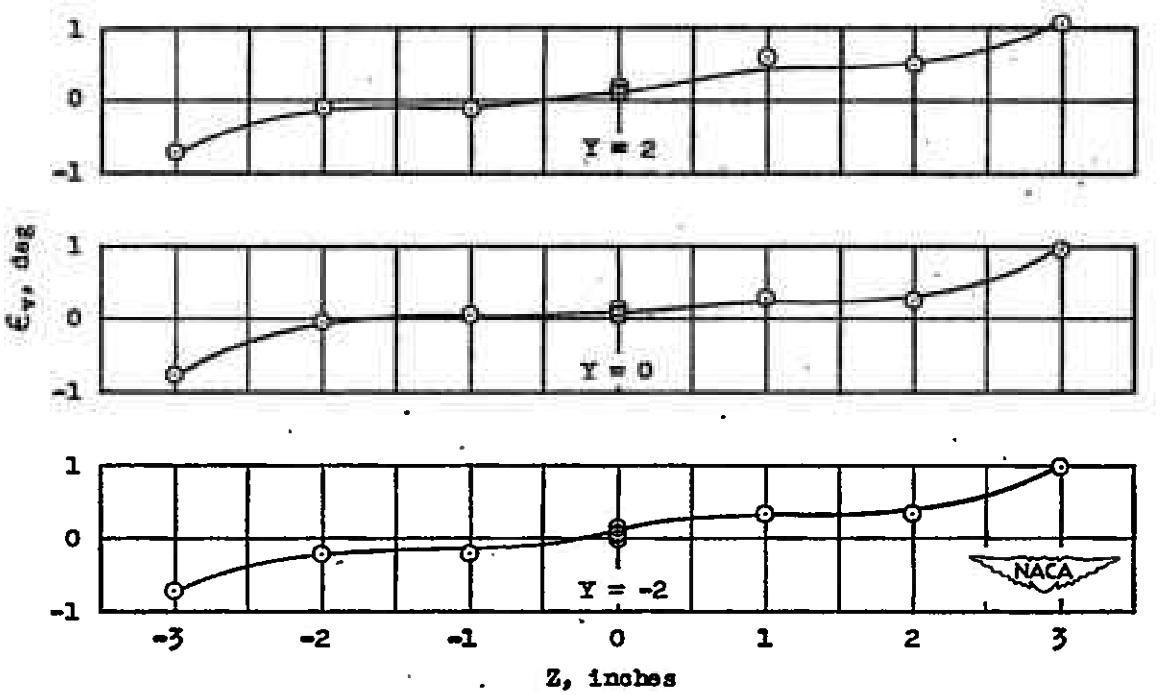

(b) Flow angle plotted against vertical station.

Figure 13.- Flow angles at X = 55.8.

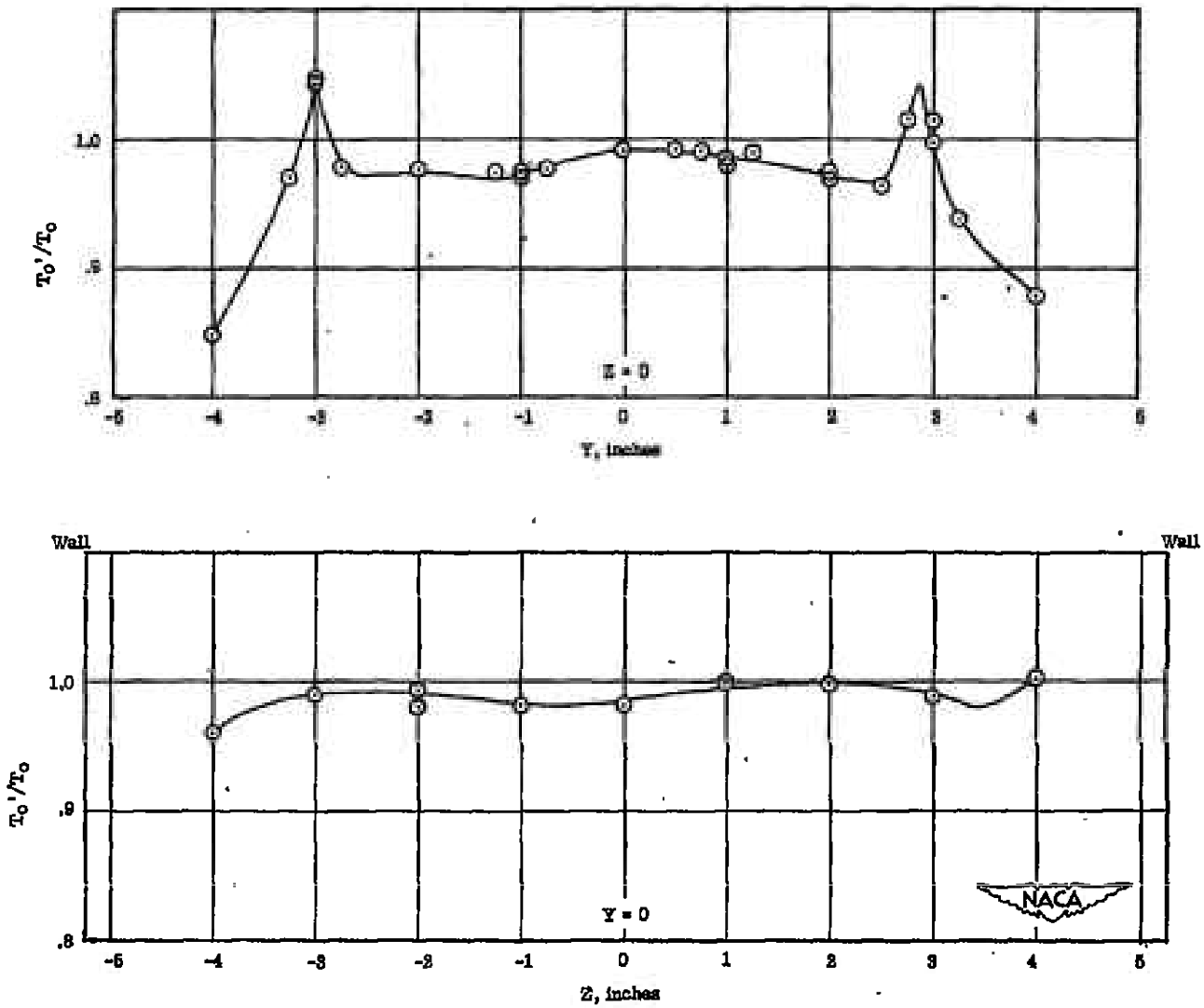

Figure 14.- Results of stagnation-temperature surveys at X = 55.8.

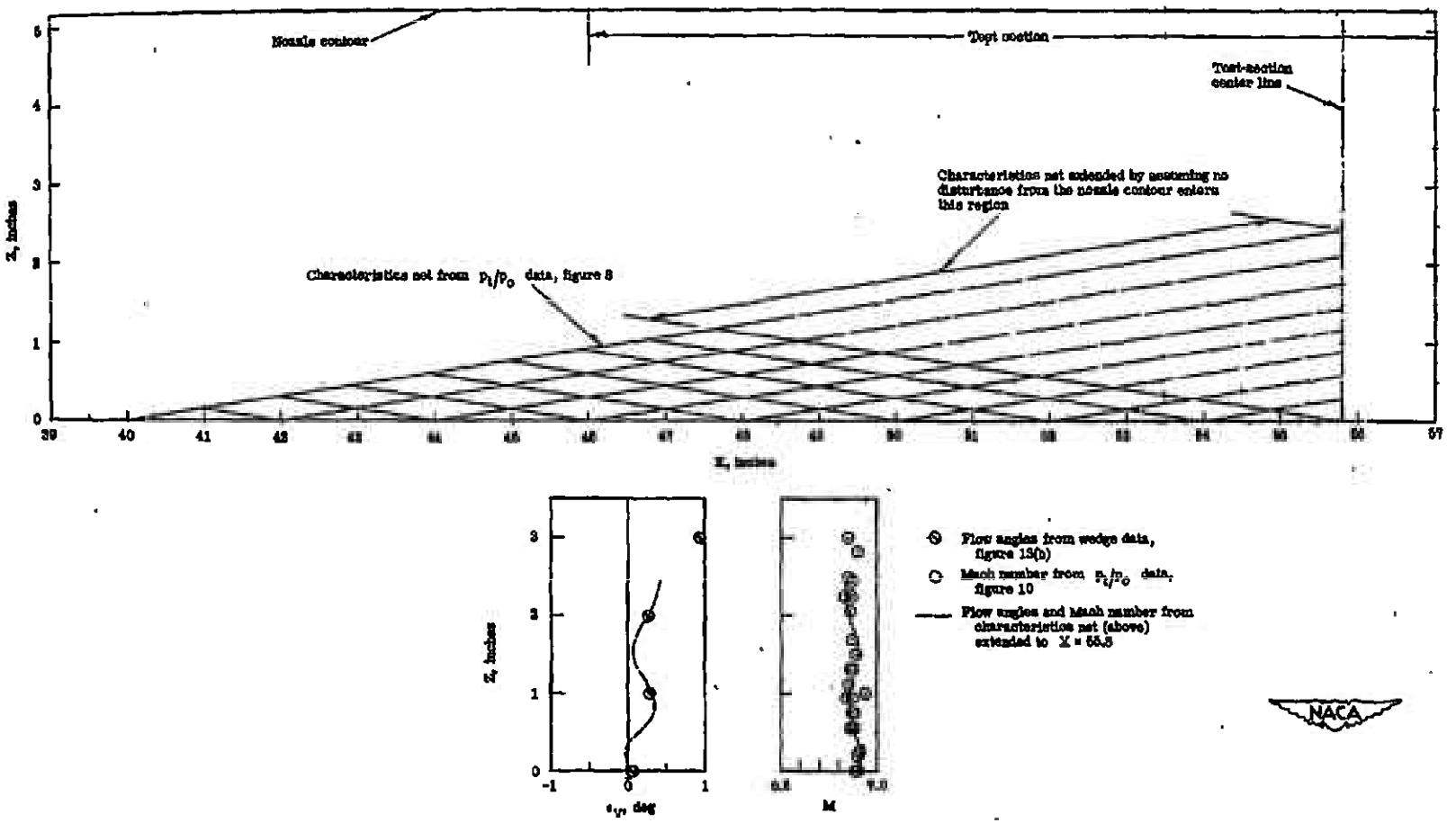

Figure 15.- Correlation of impact-pressure data along the tunnel axis with impact-pressure and flow-angle data at X = 55.8 and Y = 0 by construction of a characteristics net.